

# pH-Induced Reversible Wetting Transition between the Underwater Superoleophilicity and Superoleophobicity

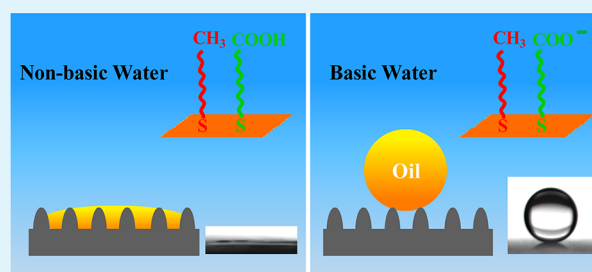
Zhongjun Cheng,<sup>†</sup> Hua Lai,<sup>†</sup> Ying Du,<sup>†</sup> Kewei Fu,<sup>†</sup> Rui Hou,<sup>†</sup> Chong Li,<sup>†</sup> Naiqing Zhang,<sup>\*,†,‡</sup> and Kening Sun<sup>\*,†,‡</sup>

<sup>‡</sup>State Key Laboratory of Urban Water Resource and Environment, School of Municipal and Environmental Engineering, and <sup>†</sup>Natural Science Research Center, Academy of Fundamental and Interdisciplinary Sciences, Harbin Institute of Technology, Harbin, Heilongjiang 150090, People's Republic of China

## S Supporting Information

**ABSTRACT:** Surfaces with controlled oil wettability in water have great potential for numerous underwater applications. In this work, we report a smart surface with pH-responsive oil wettability. The surface shows superoleophilicity in acidic water and superoleophobicity in basic water. Reversible transition between the two states can be achieved through alteration of the water pH. Such smart ability of the surface is due to the cooperation between the surface chemistry variation and hierarchical structures on the surface. Furthermore, we also extended this strategy to the copper mesh substrate and realized the selective oil/water separation on the as-prepared film. This paper reports a new surface with excellently controllable underwater oil wettability, and we believe such a surface has a lot of applications, for instance, microfluidic devices, bioadhesion, and antifouling materials.

**KEYWORDS:** *underwater superoleophilic, underwater superoleophobic, pH-responsive, oil/water separation*



## INTRODUCTION

Fishes are exceptional in their ability to keep their scales clean during swimming in oil-polluted water. This remarkable ability is ascribed to the special underwater superoleophobicity of their scales, which is resulted from the synergistic effect of hydrophilic chemical composition and hierarchical structures on their surface.<sup>1</sup> Taking the inspiration of these findings, numerous materials with such underwater superoleophobicity have been reported.<sup>2–9</sup> These novel materials could be applied in many fields, such as bioadhesion,<sup>10–12</sup> oil/water separation,<sup>13,14</sup> and microfluidic devices.<sup>15–17</sup> On the other hand, materials with underwater superoleophilicity are also attractive for application in oil absorption. Such materials have also been realized by taking advantage of the cooperation of hydrophobic/oleophilic chemical composition and the porous structures.<sup>18–30</sup> Noticeably, all of these surfaces have a constant oil wettability (superoleophilicity or superoleophobicity); surfaces with controlled oil wettability are also important because it is expected that a surface with tunable oil wettability would offer great promise for the design and fabrication of novel materials for advanced applications. Stimuli-responsive materials make it possible to reversibly control the underwater oil wettability of the surfaces and have been realized by some methods,<sup>31–36</sup> including thermal treatment,<sup>31</sup> light irradiation,<sup>8,14</sup> and the use of an electrical field.<sup>32</sup> Nevertheless, most of these works can only realize the limited transition between superoleophobicity and general oleophobicity, surfaces that can switch between the two extremes: superoleophilicity and superoleophobicity are still rare.<sup>32,33</sup>

Herein, a new surface that can switch between underwater superoleophilicity and superoleophobicity is reported. The surface is superoleophilic in nonbasic water but superoleophobic in basic water. Reversible transition between the two states can be achieved through variation of the water pH alternately. The smart ability is considered to result from the cooperation between the surface chemistry variation and rough structures on the surface. Moreover, we also extended this strategy to the copper mesh substrate and prepared a smart copper mesh film with switchable oil wettability between the two states; the special ability allows us to demonstrate a proof of selective oil/water separation via the film.

## EXPERIMENTAL SECTION

**Materials.** Poly(dimethylsiloxane) (silicon oil) and HS(CH<sub>2</sub>)<sub>9</sub>CH<sub>3</sub>, HS(CH<sub>2</sub>)<sub>10</sub>COOH, (Aldrich, Germany), (NH<sub>4</sub>)<sub>2</sub>S<sub>2</sub>O<sub>8</sub>, chloroform, NaOH, 1,2-dichloroethane, HCl, petroleum ether, *n*-hexane, methylene blue, oil red (sudan III), ethanol, and octane (Beijing Fine Chemical Co., China), and copper foils and a copper mesh substrate composed of a single layer of copper wires (99.9%, Shanghai Chemical Reagent Co., China) were used. Ultrapure water (>1.82 MΩ cm) was supplied from the Milli-Q system.

**Preparation of Rough Structures on the Substrates.** The hierarchical structures on the substrate were prepared through a method similar to that reported.<sup>37,38</sup> Briefly, the copper foils were first ultrasonically cleaned sequentially in acetone, ethanol, and water,

Received: October 26, 2013

Accepted: December 9, 2013

Published: December 9, 2013

respectively. After that, the clean copper foils were immersed in an aqueous solution of NaOH (2.5 M) and  $(\text{NH}_4)_2\text{S}_2\text{O}_8$  (0.1 M) for about 1 h. Then these substrates were taken out, washed with water, and further dried with  $\text{N}_2$ . Finally, these samples were heated at 180 °C for 2 h and further at 200 °C in  $\text{H}_2$  for about 12 h. The nanostructured copper mesh films were prepared with the same process except the immersion time was reduced to about 5 min.

**Assembly of  $\text{HS}(\text{CH}_2)_9\text{CH}_3$  and  $\text{HS}(\text{CH}_2)_{10}\text{COOH}$  on the Substrates.** Before the assembly process, a layer of gold was first coated on the substrates with a sputtercoater (Leica EM, SCDS500). After that, the substrates were immersed in a mixed thiol solution of  $\text{HS}(\text{CH}_2)_9\text{CH}_3$  and  $\text{HS}(\text{CH}_2)_{10}\text{COOH}$  for about 12 h as reported.<sup>39</sup> The ratio of  $\text{HS}(\text{CH}_2)_{10}\text{COOH}$  to  $\text{HS}(\text{CH}_2)_9\text{CH}_3$  was changed, while the whole concentration of two thiol molecules in the ethanol solution was kept constant ( $1 \text{ mmol L}^{-1}$ ). Finally, the copper substrates were taken out, rinsed with ethanol, and dried under  $\text{N}_2$ . The smooth copper surfaces and copper mesh films were modified with the same process.

**Selective Oil/Water Separation Process.** The as-prepared copper mesh film was fixed between two glass tubes, as shown in Figure 7. The mixture of oil and water was directly poured into the upper tube, and only the oil can pass through the film. If the film was first wetted by basic water ( $\text{pH} = 12$ ) and then used to separate the oil/water mixture, water can pass through the film while oil would be retained. The photographs were taken with a camera (Canon HF M41).

**Instrumentation and Characterization.** The morphology of the surface was investigated on a field-emission scanning electron microscope (Hitachi SU8010). The wettability of the surface was detected through a JC 2000D5 apparatus (Shanghai Zhongchen Digital Technology Apparatus Co., Ltd.). Before examination, the samples were first placed in a cubic and transparent quartzose container filled with ultrapure water. Oil droplets (1,2-dichloroethane and chloroform with higher density compared with water,  $4 \mu\text{L}$ ) were directly dropped onto the surfaces underwater. For oils with low density compared with water (octane and silicon oil), the surface was first fixed upside down in a quartzose container containing water, and then an inverted needle was used to place the oil droplet beneath the surface. The sliding angles were measured by tilting the sample with a  $4 \mu\text{L}$  droplet on it until the droplet started to roll. Water samples with various pH values were achieved by diluting hydrochloric acid or dissolving sodium hydroxide with water, respectively. The water pH values were determined with a pH meter (PB-10, Sartorius).

## RESULTS AND DISCUSSION

As is known, surface roughness can enhance the surface wettability, and rough structures often are necessary for the fabrication of superoleophobic and superoleophilic surfaces.<sup>1,40–48</sup> In this work, we choose copper as the substrate for its special anticorrosion property, which is important in underwater applications. The rough structure on copper foils was prepared through a sequential solution immersion, calcination, and  $\text{H}_2$  reduction process (see the Experimental Section and Supporting Information Figures S1–S3).<sup>37,38</sup> Figure 1a shows the scanning electron microscopy (SEM) image of the obtained surface. It can be seen that the surface is covered by copper nanowires and microflowers, and the microflowers with an average diameter of about  $4 \mu\text{m}$  stand on the nanowires (inset in Figure 1a). From the magnified image, one can find that the microflowers are composed of nanograins with diameters of about 80–200 nm (Figure 1b). Moreover, we can also observe that the diameters of the nanowires under the microflowers are about 20–80 nm and the whole thickness of the rough structures is about  $20 \mu\text{m}$  (see Supporting Information Figures S4 and S5). It is well-known that the hierarchical structures can amplify the wetting performance, and we hope that the hierarchical structures on

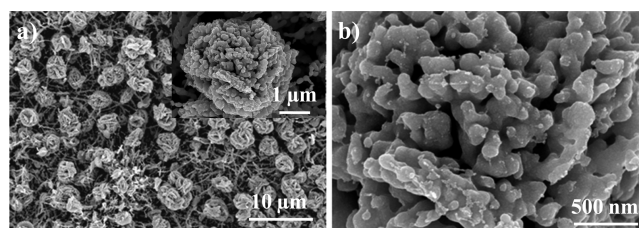


**Figure 1.** SEM images of the obtained surface at low (a) and high (b) magnification. The inset in part a is the magnified image of one microflower.

the substrate can enhance the surface oil wettability to the extremes: superoleophilicity and superoleophobicity.

To obtain the responsive surface, a stimuli-responsive molecule is necessary. As reported,<sup>49,50</sup> a carboxylic acid group can respond to the water pH. Herein two molecules,  $\text{HS}(\text{CH}_2)_9\text{CH}_3$  and  $\text{HS}(\text{CH}_2)_{10}\text{COOH}$ , containing both alkyl and carboxylic acid groups were chosen to modify the substrate.<sup>39,51,52</sup> The surface chemical composition can be controlled through changes in the ratio of the two thiol molecules in the modified solution (see Supporting Information Figures S6 and S7). We expect that the surface with such a mixed monolayer can exhibit a good pH responsivity.

By using a contact-angle admeasuring apparatus, the wetting properties of the as-prepared surfaces were investigated. Recently, Jiang et al. reported that, because of the Lewis acid/base interaction, for polar oils, even on the nonresponsive surface, the oil contact angle can be increased with increasing water pH (as to the apolar oil, the variation is unclear).<sup>34</sup> In order to exclude this influencing factor, an apolar oil octane was first chosen as the test oil. Before modification of the thiol molecules, the as-prepared hierarchical-structured copper surface is underwater superoleophobic in both acidic and basic water (see Supporting Information Figure S8), whereas after assembly of the responsive molecules, the phenomena were different, and we found that the surface prepared with  $X_{\text{COOH}} = 0.4$  ( $X_{\text{COOH}}$  is the mole fraction of the thiol molecule  $\text{HS}(\text{CH}_2)_{10}\text{COOH}$  in the mixed solution) had the most prominent pH responsivity (see Supporting Information Figure S9). Figure 2 shows the shapes of the oil droplets (octane with

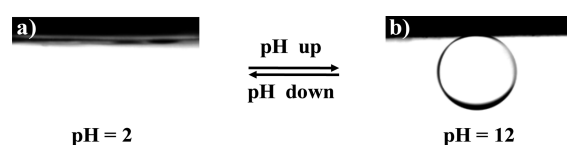


**Figure 2.** Wetting behavior of an oil droplet (octane,  $4 \mu\text{L}$ ) in contact with the hierarchical-structured surface (prepared with  $X_{\text{COOH}} = 0.4$ ) placed in acidic (a,  $\text{pH} = 2$ ) and basic (b,  $\text{pH} = 12$ ) water, respectively.

a low density compared with water) in contact with the rough surface in water. It can be seen that the surface shows superoleophilicity with a contact angle of about  $0^\circ$  (Figure 2a) in acidic water, and superoleophobicity in basic water with a contact angle of about  $162^\circ$  (Figure 2b; for more details, see Supporting Information Figure S10). Noticeably, even after immersion in water for about 24 h, the superoleophilic and superoleophobic performances can still be observed, indicating that our surface has stable superoleophilic and superoleophobic properties in water.

After being removed from the basic water, washed with pure water, and dried under  $N_2$ , the superoleophilic state can be seen again on the surface, and such a transition can be repeated several cycles without loss of responsivity (Figure 3). Noticeably, the reversibility can remain even after about 1 month, demonstrating that the as-prepared surface has a good stability.

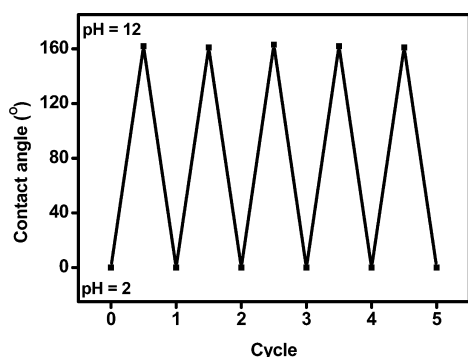


**Figure 3.** Switchable transition between underwater superoleophilicity and superoleophobicity realized by altering the water pH alternately.

In addition to the reversibility, we also investigated the relationship between the oil contact angles and water pH. As shown in Figure 4a, it can be seen that in acidic and even neutral water ( $pH \leq 7$ ) the surface shows superoleophilicity and the contact angles remain constant at about  $0^\circ$ . Upon a further increase in the water pH, the oil contact angles

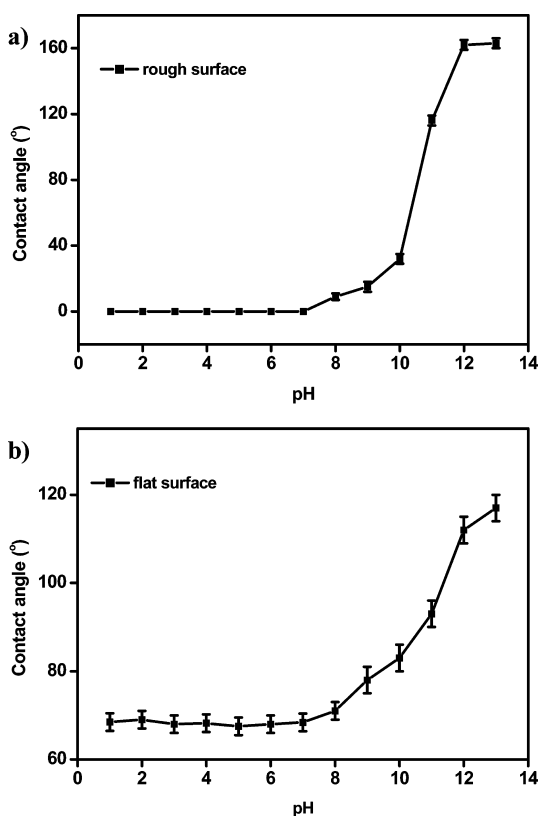


**Figure 4.** Relationship between the oil contact angle (octane,  $4 \mu\text{L}$ ) and water pH for rough (a) and flat (b) surfaces prepared with  $X_{\text{COOH}} = 0.4$ , respectively.

increased, and when the water pH was about 12, the oil contact angle increased to about  $162^\circ$  and the surface reached superoleophobicity. A similar variation trend was also observed on the flat surfaces, whereas the change was limited (Figure 4b). Moreover, some other oils, such as *n*-hexane, silicon oil, 1,2-dichloroethane, and chloroform, were also used to test the surface wettability. As shown in Figure 5, superoleophilic and

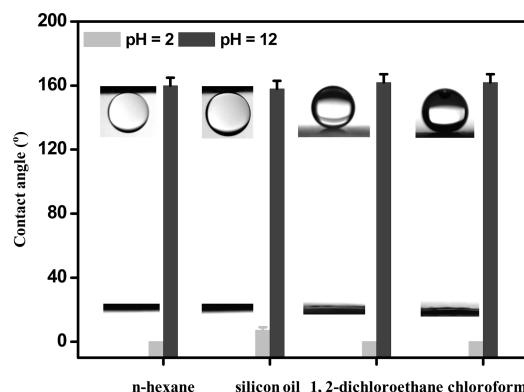


**Figure 5.** Statistics of contact angles of different oils on the surface in acidic and basic water, respectively. The insets are the wetting behaviors of an oil droplet contacting the surface under the corresponding conditions.

superoleophobic performances were also observed as the water pH was changed, indicating that the pH responsivity of our surface was universal regardless of the oil type.

To have a better understanding of the special ability of our surfaces, the mechanism that affects the oil contact angles was analyzed. When the surface was put in water, a solid/water/oil three-phase system formed, and the oil contact angle on a flat surface was calculated according to the following equation:<sup>53,54</sup>

$$\cos \theta_{ow} = \frac{\gamma_{oa} \cos \theta_o - \gamma_{wa} \cos \theta_w}{\gamma_{ow}} \quad (1)$$

Here  $\theta_o$ ,  $\theta_w$ , and  $\theta_{ow}$  are the contact angles of oil in air, water in air, and oil in water, respectively.  $\gamma_{oa}$ ,  $\gamma_{ow}$ , and  $\gamma_{wa}$  are the surface tensions of the oil/air, oil/water, and water/air interfaces. From that above, it can be found that  $\gamma_{oa}$ ,  $\gamma_{wa}$ , and  $\theta_o$  are constant when the oil type is fixed, the factors that can influence the underwater oil wettability are the water contact angle  $\theta_w$  and the oil/water surface tension  $\gamma_{ow}$ . According to Jiang et al.'s report, with increasing water pH,  $\gamma_{ow}$  can be decreased for polar oil and remain constant for apolar oil.<sup>34</sup> Thus, variation of the oil contact angles with increasing water pH, as shown in Figure 4b (the results were obtained with the apolar oil octane), can only be ascribed to variation of  $\theta_w$ . It is well-known that the surface carboxylic acid groups are protonated in nonbasic water and deprotonated in basic water, and the deprotonated state has a better hydrophilicity compared with the protonated state.<sup>39,51</sup> Thus, the water contact angles on the surface have no apparent variation before  $pH = 7$  and decrease thereafter (see Supporting Information Figure S11a). Taking the obtained water contact angles in the above equation, it would be easy to understand the phenomena shown in Figure 4b, and that is why the underwater oil contact angles have no evident change in nonbasic water and increase when the water pH increases from 7 to 13. To be specific, taking water  $pH = 2$  and 12 as examples, the octane was chosen as the oil,  $\gamma_{oa} = 21.8 \text{ mN m}^{-1}$ ,  $\gamma_{wa} = 72.0 \text{ mN m}^{-1}$ , and  $\gamma_{ow} = 51 \text{ mN m}^{-1}$ ,<sup>34</sup> and the octane contact angle

$\theta_o$  on the flat surface (prepared with  $X_{\text{COOH}} = 0.4$ ) is nearly  $0^\circ$  (Supporting Information Figure S12). The water contact angles are about  $80.5$  and  $62^\circ$  for  $\text{pH} = 2$  and  $12$ , respectively (see Supporting Information Figure S11a). According to eq 1, the calculated  $\theta_{\text{ow}}$  values are  $78$  and  $104^\circ$  in acidic and basic water, respectively, which are approximate to our experimental results (Figure 4b), indicating that the surface should be oleophilic and oleophobic in acidic and basic water, respectively. From that above, it can be found that variation of the surface chemical composition has a crucial role in changing the underwater oil wettability. Modification of the mixed thiol molecules can endow the surface with a special pH-responsive chemistry, which results in the responsive oil wettability in water (for more discussion, see Supporting Information Figure S13).

Like for the rough surface, the wetting performance can be magnified by the surface roughness. Like for acidic and neutral water, the surface shows superhydrophobicity (see Supporting Information Figure S11b). The surface cannot be wetted by water while keeping its high affinity to oil.<sup>54–58</sup> According to the Wenzel equation,<sup>54,60</sup> the rough structures on the surface can intensify the oleophilicity. As shown in Figure 1, the microflower structures and nanograins on the microflowers can contribute to the surface roughness and increase the surface area remarkably. Therefore, the oil droplet can enter into the hierarchical structures resulting from the 3D capillary effect (Figure 6a), and the surface shows underwater superoleophilicity with lower contact angles (remaining constant at about  $0^\circ$  before water  $\text{pH} = 7$ ) compared with the flat surface (Figure 4).

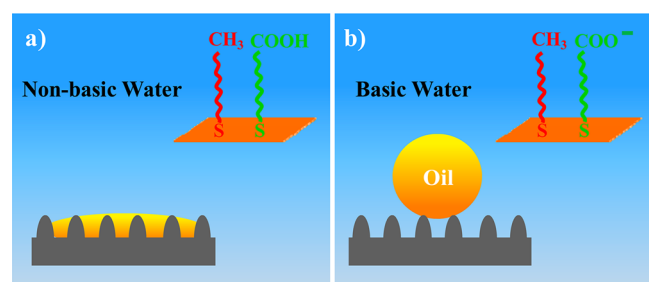


**Figure 6.** Schematic illustration of the responsive oil wettability on the rough surface: (a) in nonbasic water, the carboxylic acid groups are protonated, the surface is hydrophobic and oleophilic, and oil can enter into the microstructure and shows underwater superoleophilicity because of the 3D capillary effect; (b) in basic water, the carboxylic acid groups are deprotonated, which results in a good hydrophilicity of the surface, water can enter into the microstructure, and thus the oil droplet would reside in a composite state and show superoleophobicity.

When the water pH was increased to basic conditions, surface carboxylic acid groups were deprotonated. Hydrogen bonding between water molecules and the deprotonated carboxylic acid groups can be formed.<sup>61</sup> Meanwhile, with the presence of hierarchical structures, water was trapped among these hierarchical structures, as a result of the formation of hydrogen bonding. Thus, the oil contact angles increased because some oil/water interfaces formed between the oil droplet and solid surface. Moreover, the amount of trapped water increased as the pH was increased because more carboxylic acid groups were deprotonated. Especially when the water  $\text{pH} \geq 12$ , the amount of deprotonated carboxylic acid groups was high enough, which led to the superhydrophilicity

of the surface (see Supporting Information Figure S11b). When the surface was put in such water, the interspaces on the surface were occupied totally by water. When an oil droplet was put on the surface, it resided in a composite state (Figure 6b). The high oil contact angle can be explained by the modified Cassie equation:<sup>1,62</sup>

$$\cos \theta'_{\text{ow}} = f \cos \theta_{\text{ow}} + f - 1 \quad (2)$$

where  $f$  is the area fraction of the solid contact with the oil droplet,  $\theta'_{\text{ow}}$  is the oil contact angle on a rough solid surface in water, and  $\theta_{\text{ow}}$  is the oil contact angle on a flat solid surface in water. When the water pH is  $12$ ,  $\theta'_{\text{ow}} = 162^\circ$  (Figure 4a),  $\theta_{\text{ow}} = 112^\circ$  (Figure 4b), and  $f = 0.078$ , indicating that the surface rough structures can help to decrease the solid/oil contact area and ultimately increase the oil contact angle (according to eq 2). Therefore, the surface demonstrated superoleophobic and low-adhesive performances. After being washed with pure water and dried under  $\text{N}_2$ , the deprotonated state of carboxylic acid groups returned to the protonated state. Thus, the surface returned to the superoleophilic state in the nonbasic water, and repeated transition between the two states was achieved by altering the water pH alternately (Figure 3). From the above analysis, it was concluded that variation of the surface chemistry resulted in a change of the underwater oil wettability between the oleophilicity and oleophobicity, whereas the surface roughness effectively amplified the wetting phenomena to the two extremes: superoleophilicity and superoleophobicity.

The above explanation can help us understand the switchable transition between the superoleophilicity and superoleophobicity on the hierarchical-structured surface prepared with  $X_{\text{COOH}} = 0.4$ . Here we emphasize that the solution composition is crucial for realization of such a transition. When  $X_{\text{COOH}}$  is smaller than  $0.4$ , the obtained surfaces are mainly covered by the hydrophobic  $\text{HS}(\text{CH}_2)_9\text{CH}_3$  molecules and fewer carboxylic acid groups can be assembled. For nonbasic water, the surfaces show superhydrophobicity and underwater superoleophilicity similar to those prepared with  $X_{\text{COOH}} = 0.4$  (see Supporting Information Figure S9 and S14), while for basic water, such a small quantity of carboxylic acid groups cannot endow the surfaces with good hydrophilicity, and the obtained surfaces cannot reach superhydrophilicity (see Supporting Information Figure S14). As mentioned above, superhydrophilicity is helpful for the realization of underwater superoleophobicity. Therefore, the surfaces prepared with  $X_{\text{COOH}} < 0.4$  cannot show superoleophobicity in basic water (see Supporting Information Figure S9). When  $X_{\text{COOH}}$  is higher than  $0.4$ , the amount of carboxylic acid groups on the obtained surface would be too large. For basic water, similar to the surface prepared with  $X_{\text{COOH}} = 0.4$ , the obtained surfaces all show superhydrophilicity and underwater superoleophobicity (see Supporting Information Figures S9 and S14), while for nonbasic water, a large amount of carboxylic acid groups would lead to a decrease of the surface hydrophobicity (the surfaces cannot reach superhydrophobicity; see Supporting Information Figure S14). Thus, when these surfaces are put in the water, water can enter into the microstructures. As a result, the oil contact angles can be increased and the surfaces cannot show underwater superoleophilicity. From that above, it can be concluded that the solution composition is very important for the surface with switchable wettability between the superoleophilicity and superoleophobicity, and the solution with  $X_{\text{COOH}} = 0.4$  can provide the best pH responsivity.

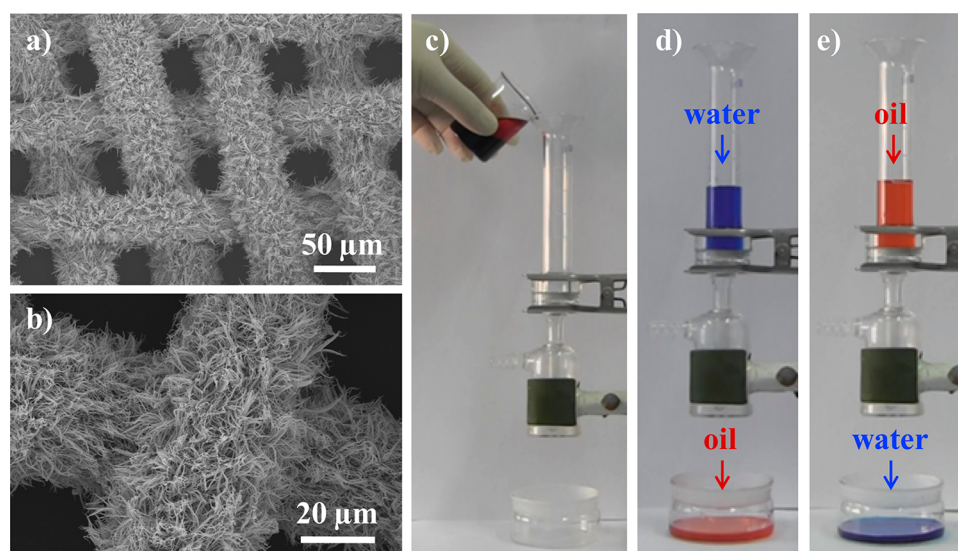


**Figure 7.** (a and b) SEM images of the nanostructured copper mesh film at different magnifications. (c) Oil/water separating device using the obtained copper mesh film as the separating membrane. (d) Oil flows into the underbottle, and water is retained on the as-prepared film. (e) When the film is first wetted by the basic water (pH = 12), water passes through the film while oil is retained.

The strategy is so simple and versatile that it can be easily extended to many other substrates, for example, the copper mesh substrates. As shown in Figure 7a,b, through a similar fabrication process, copper nanowires with diameters of about 200 nm can be produced. After modification of the mixed thiol molecules, the copper mesh film shows similar pH-responsive oil wettability (see Supporting Information Figures S15 and S16). Noticeably, such a novel film can be used in the selective oil/water separation, which has attracted much attention for lots of accidents about oil leakage.<sup>63–66</sup> Figure 7c shows a separating device using the as-prepared film as the separating membrane. For nonbasic water, the film shows superhydrophobic and superoleophilic properties (see Supporting Information Figure S16a–c). Therefore, when a mixture of water (nonbasic) and oil (petroleum ether) was poured into the glass tube above the film, only oil permeated the film and water was retained (Figure 7d; blue and red color of water and oil for the presence of methylene blue and oil red, respectively). However, when the film was first wetted by the basic water (pH = 12) and then used under the same conditions, the opposite phenomenon was observed. One finds that water passes through the film while oil is retained (Figure 7e), which can be ascribed to the superhydrophilicity (after wetting by basic water) and underwater superoleophobicity of the film (see Supporting Information Figure S16d,e). From that above, it was found that the permeation of oil or water can be selectively switched according to one's requirement on the film, and we believe that such an ability allows the film to be used in a lot of applications, for example, waste water treatment and some microfluidic devices.

## CONCLUSIONS

In summary, a smart surface with pH responsivity that can switch between underwater superoleophilicity and superoleophobicity was prepared through a simple solution immersion and thiol modification process. In nonbasic water, the surface showed underwater superoleophilicity, and in basic water, it became superoleophobic. Reversible transition between the two states was achieved by altering the water

pH alternately. The smart ability of the surface was attributed to the combined effect of the surface chemistry variation and rough structures on the surface. Moreover, we also extended the strategy to the copper mesh substrate and demonstrated a proof of selective oil/water separation on the as-prepared film. Considering that the strategy advanced here is so simple and the obtained surface is so smart, we believe the results reported in this paper could open a new perspective in controlling the surface oil wettability and have wide applications, for example, chemical engineering materials, antipollution, and microfluidic devices.

## ASSOCIATED CONTENT

### Supporting Information

SEM images of copper surface after immersion for different times and after calcinations and H<sub>2</sub> reduction and of copper nanowire under the microflower, XRD of the surface, cross-sectional view of the surface, XPS results of the surfaces, shapes of an oil droplet on the hierarchical structured copper surface in water, dependence of the oil contact angle on  $X_{\text{COOH}}$ , shape of an oil droplet rolling away from the surface in basic water, dependence of the water contact angle on the water pH for flat and rough surfaces prepared with  $X_{\text{COOH}} = 0.4$ , dependence of underwater oil contact angles on the water pH for polar oil, dependence of the contact angle on  $X_{\text{COOH}}$  for water with different pH values, dependence of the oil contact angle on  $X_{\text{COOH}}$  on the copper mesh substrate, and shapes of the water and oil droplets on copper mesh films prepared with  $X_{\text{OH}} = 0.4$  in air and water. This material is available free of charge via the Internet at <http://pubs.acs.org>.

## AUTHOR INFORMATION

### Corresponding Authors

\*E-mail: [keningsunhit@126.com](mailto:keningsunhit@126.com). Tel: (+86) 045186412153. Fax: (+86) 045186412153.

\*E-mail: [zqmw@163.com](mailto:zqmw@163.com). Tel: (+86) 045186412153. Fax: (+86) 045186412153.

### Notes

The authors declare no competing financial interest.

## ACKNOWLEDGMENTS

This work is supported by the National Natural Science Foundation of China (NSFC; Grant 21304025), Open Project of State Key Laboratory of Urban Water Resource and Environment, Harbin Institute of Technology (Grant ES201008), The Research Fund for the Doctoral Program of Higher Education of China (Grant 20112302120062), and China Postdoctoral Science Foundation (Grant 2011M500650).

## REFERENCES

- (1) Liu, M.; Wang, S.; Wei, Z.; Song, Y.; Jiang, L. *Adv. Mater.* **2009**, *21*, 665–669.
- (2) Xue, B.; Gao, L.; Hou, Y.; Liu, Z.; Jiang, L. *Adv. Mater.* **2013**, *25*, 273–277.
- (3) Xu, L.; Peng, J.; Liu, Y.; Wen, Y.; Zhang, X.; Jiang, L.; Wang, S. *ACS Nano* **2013**, *7*, 5077–5083.
- (4) Xu, L.; Zhao, J.; Su, B.; Liu, X.; Peng, J.; Liu, Y.; Liu, H.; Yang, G.; Jiang, L.; Wen, Y.; Zhang, X.; Wang, S. *Adv. Mater.* **2013**, *25*, 606–611.
- (5) Liu, X.; Zhou, J.; Xue, Z.; Gao, J.; Meng, J.; Wang, S.; Jiang, L. *Adv. Mater.* **2012**, *24*, 3401–3405.
- (6) Xue, Z.; Liu, M.; Jiang, L. *J. Polym. Sci., Polym. Phys.* **2012**, *50*, 1209–1224.
- (7) Lin, L.; Liu, M.; Chen, L.; Chen, P.; Ma, J.; Han, D.; Jiang, L. *Adv. Mater.* **2010**, *22*, 4826–4830.
- (8) Sawai, Y.; Nishimoto, S.; Kameshima, Y.; Fujii, E.; Miyake, M. *Langmuir* **2013**, *29*, 6784–6789.
- (9) Cheng, Z.; Lai, H.; Fu, K.; Zhang, N.; Sun, K. *Chem. J. Chin. Univ.* **2013**, *34*, 2778–2782.
- (10) Sheparovych, R.; Motornov, M.; Minko, S. *Adv. Mater.* **2009**, *21*, 1840–1844.
- (11) Chen, L.; Liu, M.; Bai, H.; Chen, P.; Xia, F.; Han, D.; Jiang, L. *J. Am. Chem. Soc.* **2009**, *131*, 10467–10472.
- (12) Wischerhoff, E.; Uhlig, K.; Lankeau, A.; Börner, H. G.; Laschewsky, A.; Duschl, C.; Lutz, J.-F. *Angew. Chem., Int. Ed.* **2008**, *47*, 5666–5668.
- (13) Xue, Z.; Wang, S.; Lin, L.; Chen, L.; Liu, M.; Feng, L.; Jiang, L. *Adv. Mater.* **2011**, *23*, 4270–4273.
- (14) Tian, D.; Zhang, X.; Tian, Y.; Wu, Y.; Wang, X.; Zhai, J.; Jiang, L. *J. Mater. Chem.* **2012**, *22*, 19652–19657.
- (15) Wu, D.; Wu, S.; Chen, Q.; Zhao, S.; Zhang, H.; Jiao, J.; Piersol, J. A.; Wang, J.; Sun, H.; Jiang, L. *Lab Chip* **2011**, *11*, 3873–3879.
- (16) Ionov, L.; Houbenkov, N.; Sidorenko, A.; Stamm, M.; Minko, S. *Adv. Funct. Mater.* **2006**, *16*, 1153–1160.
- (17) Truman, P.; Uhlmann, P.; Frenzel, R.; Stamm, M. *Adv. Mater.* **2009**, *21*, 3601–3604.
- (18) Guix, M.; Orozco, J.; García, M.; Gao, W.; Sattayasamitsathit, S.; Merkoci, A.; Escarpa, A.; Wang, J. *ACS Nano* **2012**, *6*, 4445–4451.
- (19) Zhu, Q.; Pan, Q.; Liu, F. *J. Phys. Chem. C* **2011**, *115*, 17464–17470.
- (20) Wu, J.; Wang, N.; Wang, L.; Dong, H.; Zhao, Y.; Jiang, L. *ACS Appl. Mater. Interfaces* **2012**, *4*, 3207–3212.
- (21) Venkataraman, P.; Tang, J.; Frenkel, E.; McPherson, G. L.; He, J.; Raghavan, S. R.; Kolesnichenko, V.; Bose, A.; John, V. T. *ACS Appl. Mater. Interfaces* **2013**, *5*, 3572–3580.
- (22) Bi, H.; Xie, X.; Yin, K.; Zhou, Y.; Wan, S.; He, L.; Xu, F.; Banhart, F.; Sun, L.; Ruoff, R. S. *Adv. Funct. Mater.* **2012**, *22*, 4421–4425.
- (23) Deng, D.; Prendergast, D. P.; MacFarlane, J.; Bagatin, R.; Stellacci, F.; Gschwend, P. M. *ACS Appl. Mater. Interfaces* **2013**, *5*, 774–781.
- (24) Li, S.; Jiao, X.; Yang, H. *Langmuir* **2013**, *29*, 1228–1237.
- (25) Wang, C.; Tzeng, F.; Chen, H.; Chang, C. *Langmuir* **2012**, *28*, 10015–10019.
- (26) Calcagnile, P.; Fragouli, D.; Bayer, I. S.; Anyfantis, G. C.; Martiradonna, L.; Cozzoli, P. D.; Cingolani, R.; Athanassiou, A. *ACS Nano* **2012**, *6*, 5413–5419.
- (27) Cheng, M.; Gao, Y.; Guo, X.; Shi, Z.; Chen, J.; Shi, F. *Langmuir* **2011**, *27*, 7371–7375.
- (28) Zhang, Y.; Wei, S.; Liu, F.; Du, Y.; Liu, S.; Ji, Y.; Yokoi, T.; Tatsumi, T.; Xiao, F. *Nano Today* **2009**, *4*, 135–142.
- (29) Yuan, J.; Liu, X.; Akbulut, O.; Hu, J.; Suib, S. L.; Kong, J.; Stellacci, F. *Nat. Nanotechnol.* **2008**, *3*, 332–336.
- (30) Jin, M.; Wang, J.; Yao, X.; Liao, M.; Zhao, Y.; Jiang, L. *Adv. Mater.* **2011**, *23*, 2861–2864.
- (31) Chen, L.; Liu, M.; Lin, L.; Zhang, T.; Ma, J.; Song, Y.; Jiang, L. *Soft Matter* **2010**, *6*, 2708–2712.
- (32) Liu, M.; Liu, X.; Ding, C.; Wei, Z.; Zhu, Y.; Jiang, L. *Soft Matter* **2011**, *7*, 4163–4165.
- (33) Zhang, L.; Zhang, Z.; Wang, P. *NPG Asia Mater.* **2012**, *4*, e8.
- (34) Liu, M.; Xue, Z.; Liu, H.; Jiang, L. *Angew. Chem., Int. Ed.* **2012**, *51*, 8348–8351.
- (35) Ding, C.; Zhu, Y.; Liu, M.; Feng, L.; Wan, M.; Jiang, L. *Soft Matter* **2012**, *8*, 9064–9068.
- (36) Cheng, Q.; Li, M.; Yang, F.; Liu, M.; Li, L.; Wang, S.; Jiang, L. *Soft Matter* **2012**, *8*, 6740–6743.
- (37) Zhu, X.; Zhang, Z.; Men, X.; Yang, J.; Xu, X. *ACS Appl. Mater. Interfaces* **2010**, *2*, 3636–3641.
- (38) Chen, X.; Kong, L.; Dong, D.; Yang, G.; Yu, L.; Chen, J.; Zhang, P. *J. Phys. Chem. C* **2009**, *113*, 5396–5401.
- (39) Yu, X.; Wang, Z. Q.; Jiang, Y. G.; Shi, F.; Zhang, X. *Adv. Mater.* **2005**, *17*, 1289–1293.
- (40) Hancock, M. J.; Sekeroglu, K.; Demirel, M. C. *Adv. Funct. Mater.* **2012**, *22*, 2223–2234.
- (41) Xiu, Y.; Zhu, L.; Hess, D. W.; Wong, C. P. *Nano Lett.* **2007**, *7*, 3388–3393.
- (42) Ming, W.; Wu, D.; van Benthem, R.; de With, G. *Nano Lett.* **2005**, *5*, 2298–2301.
- (43) Zhang, X.; Shi, F.; Niu, J.; Jiang, Y.; Wang, Z. *J. Mater. Chem.* **2008**, *18*, 621–633.
- (44) Roach, P.; Shirtcliffe, N. J.; Newton, M. I. *Soft Matter* **2008**, *4*, 224–240.
- (45) Lafuma, A.; Quéré, D. *Nat. Mater.* **2003**, *2*, 457–460.
- (46) Blossey, R. *Nat. Mater.* **2003**, *2*, 301–306.
- (47) Li, X. M.; Reinhoudt, D.; Crego-Calama, M. *Chem. Soc. Rev.* **2007**, *36*, 1350–1368.
- (48) Cheng, Z.; Du, M.; Lai, H.; Zhang, N.; Sun, K. *Chem. J. Chin. Univ.* **2013**, *34*, 606–609.
- (49) Hou, X.; Liu, Y.; Dong, H.; Yang, F.; Li, L.; Jiang, L. *Adv. Mater.* **2010**, *22*, 2440–2443.
- (50) Liu, D.; Liu, H.; Hu, N. *Electrochim. Acta* **2010**, *55*, 6426–6432.
- (51) Bain, C. D.; Whitesides, G. M. *Langmuir* **1989**, *5*, 1370–1378.
- (52) Ulman, A. *Chem. Rev.* **1996**, *96*, 1533–1554.
- (53) Jung, Y. C.; Bhushan, B. *Langmuir* **2009**, *25*, 14165–14173.
- (54) Hejazi, V.; Nosonovsky, M. *Langmuir* **2012**, *28*, 2173–2180.
- (55) Jin, M.; Li, S.; Wang, J.; Xue, Z.; Liao, M.; Wang, S. *Chem. Commun.* **2012**, *48*, 11745–11747.
- (56) Luo, C.; Zheng, H.; Wang, L.; Fang, H.; Hu, J.; Fan, C.; Cao, Y.; Wang, J. *Angew. Chem., Int. Ed.* **2010**, *49*, 9145–9148.
- (57) Bobji, M. S.; Kumar, S. V.; Asthana, A.; Govardhan, R. N. *Langmuir* **2009**, *25*, 12120–12126.
- (58) Marmur, A. *Langmuir* **2006**, *22*, 1400–1402.
- (59) Poetes, R.; Holtzmann, K.; Franze, K.; Steiner, U. *Phys. Rev. Lett.* **2010**, *105*, 166104.
- (60) Wenzel, R. N. *Ind. Eng. Chem.* **1936**, *28*, 988–994.
- (61) Xia, F.; Feng, L.; Wang, S.; Sun, T.; Song, W.; Jiang, W.; Jiang, L. *Adv. Mater.* **2006**, *18*, 432–436.
- (62) Cassie, A. B. D.; Baxter, S. *Trans. Faraday Soc.* **1944**, *40*, 546–551.
- (63) Zhang, F.; Zhang, W. B.; Shi, Z.; Wang, D.; Jin, J.; Jiang, L. *Adv. Mater.* **2013**, *25*, 4192–4198.
- (64) Shannon, M. A.; Bohn, P. W.; Elimelech, M.; Georgiadis, J. G.; Marinas, B. J.; Mayes, A. M. *Nature* **2008**, *452*, 301–310.
- (65) Lahann, J. *Nat. Nanotechnol.* **2008**, *3*, 320–321.
- (66) Han, Y.; Xu, Z.; Gao, C. *Adv. Funct. Mater.* **2013**, *23*, 3693–3700.